









The neural pathway of the hyperthermic response to antagonists of the transient receptor potential vanilloid-1 channel

Andras Garami ^{a,b}, Alexandre A. Steiner ^{a,c}, Eszter Pakai^{a,b}, Samuel P. Wanner ^a, M. Camila Almeida ^a, Patrik Keringer ^b, Daniela L. Oliveira^a, Kazuhiro Nakamura ^d, Shaun F. Morrison ^e, and Andrej A. Romanovsky ^{a,f,g}

^aThermoregulation and Systemic Inflammation Laboratory (FeverLab), St. Joseph's Hospital and Medical Center, Phoenix, AZ, USA; ^bDepartment of Thermophysiology, Institute for Translational Medicine, Medical School, University of Pecs, Pecs, Hungary; ^cDepartamento de Imunologia, Instituto de Ciencias Biomedicas, Universidade de Sao Paulo, São Paulo, Brazil; ^dDepartment of Integrative Physiology, Nagoya University Graduate School of Medicine, Nagoya, Japan; ^eDepartment of Neurological Surgery, Oregon Health and Science University, Portland, OR, USA; ^fSchool of Molecular Sciences, University of Arizona, Tempe, AZ, USA; ^gZharko Pharma, Inc., Olympia, WA, USA

ABSTRACT

We identified the neural pathway of the hyperthermic response to TRPV1 antagonists. We showed that hyperthermia induced by i.v. AMG0347, AMG 517, or AMG8163 did not occur in rats with abdominal sensory nerves desensitized by pretreatment with a low i.p. dose of resiniferatoxin (RTX, TRPV1 agonist). However, neither bilateral vagotomy nor bilateral transection of the greater splanchnic nerve attenuated AMG0347-induced hyperthermia. Yet, this hyperthermia was attenuated by bilateral high cervical transection of the spinal dorsolateral funiculus (DLF). To explain the extra-splanchnic, spinal mediation of TRPV1 antagonist-induced hyperthermia, we proposed that abdominal signals that drive this hyperthermia originate in skeletal muscles – not viscera. If so, in order to prevent TRPV1 antagonist-induced hyperthermia, the desensitization caused by i.p. RTX should spread into the abdominal-wall muscles. Indeed, we found that the local hypoperfusion response to capsaicin (TRPV1 agonist) in the abdominal-wall muscles was absent in i.p. RTX-desensitized rats. We then showed that the most upstream (lateral parabrachial, LPB) and the most downstream (rostral raphe pallidus) nuclei of the intrabrain pathway that controls autonomic cold defenses are also required for the hyperthermic response to i.v. AMG0347. Injection of muscimol (inhibitor of neuronal activity) into the LPB or injection of glycine (inhibitory neurotransmitter) into the raphe blocked the hyperthermic response to i.v. AMG0347, whereas i.v. AMG0347 increased the number of c-Fos cells in the raphe. We conclude that the neural pathway of TRPV1 antagonist-induced hyperthermia involves TRPV1-expressing sensory nerves in trunk muscles, the DLF, and the same LPB-raphe pathway that controls autonomic cold defenses.

ARTICLE HISTORY

Received 22 October 2022
Revised 13 January 2023
Accepted 18 January 2023

KEYWORDS

Thermoregulation; TRPV1 blockers; hyperthermia; protons; vagus; splanchnic; spinal cord; skeletal muscle

Introduction

Many antagonist of the transient receptor potential (TRP) cation channel subfamily V member 1 (TRPV1) cause an increase in deep body temperature (T_b), an effect observed in a variety of species, including humans (for review, see [1,2]), and occurring due to increased thermogenesis and cutaneous vasoconstriction [3,4]. It is thought that TRPV1 channels are normally tonically activated by protons (low pH), and that this tonic activation contributes to the maintenance of normal T_b through the suppression of autonomic cold-defense effectors (thermogenesis and skin vasoconstriction) via the proposed acido-antithermogenic and acido-antivasonconstrictor reflexes

[1]. When a TRPV1 antagonist blocks tonic proton activation of TRPV1 channels, this disinhibits thermogenesis and cutaneous vasoconstriction, and hyperthermia occurs.

The intraperitoneal (i.p.) pretreatment of rats with a low dose of the TRPV1 agonist resiniferatoxin (RTX, 20 $\mu\text{g}/\text{kg}$), which causes localized functional impairment (*i.e.*, desensitization) of abdominal TRPV1 channels [4,5], was reported to abolish hyperthermic responses to AMG0347 [4] and A889425 [6]. These results suggest that acido-antithermogenic and acido-antivasonconstrictor reflexes originate at a tonically active TRPV1 population somewhere in the abdomen, perhaps in the abdominal viscera or in skeletal muscles of the

trunk [2]. The exact location of this TRPV1 population is unknown, but it is associated with sensory nerves rather than vasculature [7]; it is also unknown what neural pathways form the substrate of the acido-antithermogenic and acido-antivasconstrictor reflexes.

The abdominal viscera are serviced by the vagus nerve and several splanchnic nerves, including thoracic (greater, lesser, least), lumbar, and pelvic [8–10]. TRPV1 channels are expressed on all these afferents [11–14]. TRPV1 channels are also expressed in multiple skeletal muscles in rats and mice [15–18] and in the rectus abdominis muscle in humans [15]. Skeletal muscles are innervated by somatic nerves, and afferent fibers sensitive to capsaicin (the “classical” TRPV1 agonist [19]) have also been demonstrated in skeletal muscles in rats and dogs [20,21].

The present study aimed at identifying the neural pathway of TRPV1 antagonist-induced hyperthermia in rats. Using multiple experimental paradigms and approaches, we attempted to establish whether this pathway originates in the abdominal viscera or muscles, whether it travels through the vagal or spinal afferents, and how it converges with the known thermoeffector pathways.

Materials and methods

Animals

The experiments were conducted in 174 adult male Wistar rats. Of these, 123 rats (360 ± 31 g) were obtained from Harlan and used in thermophysiological experiments in unanesthetized animals at St. Joseph’s Hospital and Medical Center. Thirty-seven rats (340 ± 63 g) were obtained from the Laboratory Animal Centre of the University of Pecs, where they were used for skeletal-muscle blood-perfusion measurements in anesthetized animals. Fourteen rats (393 ± 66 g) were purchased from Charles River Laboratories and used in electrophysiological experiments in anesthetized animals at Oregon Health and Science University. At all three centers, rats were housed in temperature-controlled rooms on a 12 h light/dark cycle. Standard rodent chow and tap water were available *ad libitum*, except for some procedures

associated with vagotomy and splanchnicotomy (for details, see Surgeries below).

At St. Joseph’s Hospital and Medical Center, rats were extensively handled and then habituated to staying inside wire-mesh cylindrical confinements. The cylindrical confinements prevented rats from turning around but allowed for some back-and-forth movements; they were used in thermophysiological experiments (see Experimental protocols below).

All procedures at each center were conducted under protocols approved by its Institutional Animal Use and Care Committee.

Surgeries

Each rat designated to the thermophysiological experiments received either a surgical (total subdiaphragmatic truncal vagotomy, bilateral splanchnicotomy, bilateral cervical funiculotomy) or pharmacological (for details, see Abdominal TRPV1 desensitization) neural lesioning procedure or the corresponding sham-lesioning procedure, as described below. The lesioning procedure was performed 7–23 d before an experiment. After the animals recovered from the neural lesioning procedure, an intravenous (i.v.) catheter for drug delivery was implanted in the left jugular vein (4–8 d before the experiment).

All surgeries were conducted under anesthesia induced by i.p. administration of a ketamine-xylazine-acepromazine cocktail (55.6, 5.5, and 1.1 mg/kg, respectively) and under antibiotic protection (enrofloxacin, 1.1 mg/kg, subcutaneously).

Total subdiaphragmatic truncal vagotomy. This surgical procedure has been described in detail elsewhere [22,23]. In short, following an overnight food deprivation, a rat was anesthetized, and the stomach was accessed via a middle upper laparotomy and gently pulled to expose the esophagus. The ventral and dorsal vagal trunks running along the esophagus were identified and cut immediately below the diaphragm; for certainty, the hepatic vagal branch was also cut separately. In sham-vagotomized rats, the viscera were handled, but no nerves were cut. To alleviate the gastrointestinal complications of vagotomy, vagotomized (but not sham-vagotomized) rats were offered a highly

palatable liquid diet (PMI Micro-stabilized Rodent Liquid Diet LD101; TestDiet) for 9 days following the surgery [23]. In vagotomized animals, the stomach size greatly increases due to food retention, as a result of decreased gastrointestinal tone and motility [24,25]. Hence, the completeness of vagotomy was confirmed by weighing the stomach of the rats at the end of the experiments, as in our earlier studies [23,26].

Bilateral splanchnicotomy. A midline laparotomy was performed, and the stomach and liver were deflected from the subdiaphragmatic area with saline-moistened gauze to expose the dorsal abdominal wall. On each side, the retroperitoneal space was opened, and the greater splanchnic nerve was isolated and cut, either as a single trunk or as two or more divisions, just beneath the diaphragm as in our earlier study [27]. In sham splanchnicotomy, the nerve was exposed on each side but not cut. The integrity of the greater splanchnic nerve is required for the modulation of adrenal responsiveness [28]. The adrenal splanchnic innervation is an additional mechanism controlling the production of corticosterone independently from adrenocorticotrophic hormone, and splanchnicotomized rats were shown to express an attenuated corticosterone response to water deprivation [29]. To verify the completeness of splanchnicotomy, at the end of the experiments, rats were subjected to a 48-h water deprivation and then anesthetized, and their arterial blood was collected by cardiac puncture in a heparin-containing Vacutainer tube and centrifuged (3000 g, 10 min, 4°C). The plasma corticosterone concentration was measured by ELISA (Assay Designs).

Bilateral cervical funiculotomy. This surgery was performed as described in a parallel study in our laboratory [30]. The skin over the upper back, neck, and head was shaved and scrubbed. The skin was incised over the vertebral column at the level of the first and second cervical vertebrae (C1 and C2, respectively), and the underlying muscles were retracted. A partial laminectomy was performed at the C1 level to expose the spinal cord from a dorsal approach. Then, the dura mater was cut with eye scissors, thus opening the subdural space. Next, a micro knife was used to make a shallow transversal incision aimed at transecting

the dorsal aspect of the lateral funiculus (dorsolateral funiculus, DLF) at C1. These procedures were performed bilaterally. A fat pad was inserted in the laminectomy defect, and muscles and skin were sutured in layers. After the thermophysiological experiments were completed, the successful interruption of ascending nociceptive pathways was confirmed in each rat by immersing its tail into a 75% ethanol solution in water (−18°C) and measuring the latency of the tail-flick response [30]. In each rat, the completeness of the bilateral lesion of the DLF was verified histologically, as described by Vizin et al. [30]; only rats having a lesion covering >50% of the targeted area on each side of the spinal cord at C1 were considered to have a “complete” lesion.

Intravenous catheterization. The left jugular vein was exposed, freed from its surrounding connective tissue, and ligated. A silicone catheter (ID 0.5 mm, OD 0.9 mm) filled with heparinized (10 U/ml) saline was passed into the superior vena cava through the jugular vein and secured in place with ligatures. The free end of the catheter was knotted, tunneled under the skin to the nape of the neck, and exteriorized. The wound was sutured in layers. The catheter was flushed with heparinized saline (10 U/ml) every other day.

Abdominal TRPV1 desensitization

This procedure was performed in rats that were used for the thermophysiological experiments or skeletal-muscle blood-perfusion measurements.

To cause localized (abdominal) desensitization of TRPV1 channels, rats were injected i.p. with 20 µg/kg RTX. This relatively low dose of RTX was shown to selectively impair the function of TRPV1 channels within the abdominal cavity [4–6,31]. As in the past, we confirmed a functional impairment of TRPV1 channels in the peritoneal cavity by counting the number of writhing episodes for 10 min following injection of RTX (0.1 µg/kg, i.p.) [4,31]. To verify that the desensitizing effect did not spread beyond the abdomen, we compared TRPV1-mediated responses to an extra-abdominal stimulus by applying to the cornea 20 µl of RTX solution (2 µg/ml) at St. Joseph’s Hospital and Medical Center or 40 µl of capsaicin solution (10 µg/ml) at University of Pecs, and

counting the eye-wiping movements for 5 min or 1 min, respectively. Experiments in rats with localized abdominal TRPV1 desensitization were conducted 7–14 days after the i.p. administration of RTX.

Experimental protocols

Thermophysiological experiments in unanesthetized rats. A thermocouple thermometry setup or thermocouple thermometry-respirometry setup [4,32] was used. In either setup, each rat was loosely restrained with an individual confiner and had a copper-constantan colonic thermocouple (Omega Engineering) inserted in the colon, 10 cm beyond the anal sphincter, to measure colonic temperature (a measure of deep T_b). In a subset of experiments, oxygen consumption (VO_2 , a measure of thermogenesis) was recorded by a multi-channel respirometer (Sable Systems). For that, rats in their confiners were placed inside cylindrical Plexiglas chambers (Sable Systems), which were sealed and continuously ventilated. The airflow was maintained at 600 ml/min with a mass flow controller (Sierra Instruments). Air leaving the chambers was automatically sampled, dried, and passed through an oxygen analyzer (Sable Systems). In either setup, the rats were kept inside a climatic chamber (model 3940; Forma Scientific); the ambient temperature inside the climatic chamber was recorded with thermocouples connected to a data logger (Cole-Parmer). The venous catheter was connected to a PE-50 extension filled with the drug or the vehicle. When a respirometry chamber was present, the extension was passed through its port, which was then sealed with paraffin. The extension was passed through a port of the climatic chamber and connected to a syringe placed in an infusion pump (model 220, KD Scientific), thus allowing the drug to be administered without disturbing the animal. Each experiment was conducted under thermoneutral conditions determined for the experimental setups in earlier studies [4,33].

Blood-perfusion measurements in anesthetized rats. The rats were anesthetized with i.p. administration of a ketamine-xylazine cocktail (78 and 13 mg/kg, respectively); then the fur on the abdomen was clipped. A midline incision was made through the skin, and abdominal muscles were

exposed from the metasternum to 1.5 cm above the pubic arch. The animal was placed in a supine position on a heating pad (model TMP-5a; Supertech Instruments UK Ltd) to maintain the deep T_b at 35–36°C (with mean \pm standard deviation of $35.4 \pm 0.4^\circ\text{C}$) for the duration of the experiment. The limbs were fixed to the pad with adhesive tape. To reduce the movements of the abdominal wall due to breathing, the peritoneal cavity was inflated with air (400 ml/kg) with a syringe piercing the right iliac region. The abdominal-muscle surface was wiped with 0.1 ml paraffin to protect the tissue from drying. A needle injector [model 304H28RW (ID 0.18 mm, OD 0.36 mm); MicroGroup] was connected to a PE-50 extension, which was prefilled with a solution of capsaicin (6 mg/ml) or vehicle. The tip of the needle injector was inserted between the external and internal oblique abdominal muscle and positioned 0.5 cm left of the linea alba and 3 cm above the pubic arch. The blood flow in the abdominal muscle of the rat was measured by a PeriCam PSI system (Perimed AB), which applies laser speckle contrast analysis technology. Similarly to our recent study [34], the change in blood perfusion (recorded in arbitrary perfusion units) during the experiments was expressed as the difference from the baseline value recorded before the drug (or vehicle) administration. To study whether the changes in muscle perfusion occurring in response to the intramuscular (i.m.) administration of capsaicin were due to systemic hemodynamic effects, blood pressure in the left carotid artery was continuously recorded in three randomly selected sham-desensitized rats. For this, signals from a pressure transducer connected to a carotid cannula were sent to a PowerLab data acquisition system (ADInstruments).

Electrophysiological experiments in anesthetized rats. Rats were anesthetized initially with 2.5% isoflurane in 100% O_2 for the following surgical procedures. A femoral artery and vein and the trachea were cannulated. Rats were positioned prone in a stereotaxic frame with a spinal clamp on the tenth thoracic vertebra. To measure deep T_b and brown adipose tissue (BAT) temperature (T_{BAT}), thermocouples were placed 6-cm deep into the colon and into the left interscapular BAT pad, respectively, and then connected to a thermocouple meter (TC-2000, Sable

Systems International). T_b was maintained at $\sim 37.0^\circ\text{C}$ with a water jacket wrapped around the trunk and perfused with warm water as required. Postganglionic sympathetic nerve activity (SNA) to BAT was recorded from the central cut end of a small nerve bundle dissected from the ventral surface of the right interscapular BAT pad after dividing the fat pad along the midline and reflecting it laterally. Nerve activity was recorded with bipolar hook electrodes (90% platinum, 10% iridium), filtered (1–300 Hz), and amplified (50,000 \times ; Cyberamp 380, Axon Instruments). After rats were transitioned to inactin (thiobutabarbital sodium salt hydrate, 150 mg/kg, i.v.), had artificial pneumothorax induced, and paralyzed with D-tubocurarine (0.3 mg initial dose, 0.1 mg/h supplements), they were artificially ventilated with O_2 -enriched room air (60 cycles/min, tidal volume 3.0–4.5 ml). Small adjustments in minute ventilation were made as necessary to maintain basal mixed-expired CO_2 levels between 3.0 and 4.5%. AMG0347 (500 $\mu\text{g}/\text{kg}$, i.v.) was administered over 2 minutes, and the physiological variables were monitored for the subsequent hour. BAT SNA and T_{BAT} were digitized (Micro 1401 MKII; Cambridge Electronic Design) and recorded onto a computer hard drive. Spike 2 software (Cambridge Electronic Design) was used to obtain a continuous measure (4 s bins) of BAT SNA amplitude by calculating the root mean square (rms) amplitude of the BAT SNA (square root of the total power in the 0.1 to 20 Hz band) from the autospectra of sequential 4-s segments of BAT SNA. The control value of BAT SNA was the average of the BAT SNA amplitudes during the 2-min period (*i.e.*, 30 bins of BAT SNA) prior to AMG0347 treatment, and the peak effect was the average of the BAT SNA amplitudes during the 2-min period of the maximal increase in BAT SNA following AMG0347 injection; the treatment-evoked changes in T_{BAT} were calculated as the differences between these two values. Due to the variability in BAT SNA recordings (nerve bundle size, nerve contact with recording hooks, etc.) among rats, the calculated values for the BAT SNA following AMG0347 treatment are expressed as percentages of the baseline, minimum level of BAT SNA when the rat was warmed (deep $T_b > 37.0^\circ\text{C}$).

To inhibit local neurons in the lateral parabrachial nucleus (LPB), the GABA_A receptor agonist, muscimol was microinjected bilaterally (13.7 ng, 60 nl each) [35]. Chemical inactivation of neurons

in the midline of the rostral raphe pallidus nucleus (rRPa, 2.3 mm posterior to the interaural line, on the midline, and 9.5–9.7 mm ventral to the brain surface) was accomplished by single microinjections of glycine (2.3 μg , 60 nl) [36].

Drugs

Three highly potent TRPV1 antagonists, *viz.*, AMG0347 (Medkoo Biosciences), AMG 517 (Selleckchem), and AMG8163 (Medkoo Biosciences), were used; each of them has IC_{50} values ≤ 1.5 nM at blocking all three activation modes of TRPV1 [2,37]. AMG0347 was used in our earlier studies [4,37,38]. The compounds were dissolved in 100% ethanol, and aliquots of the ethanolic stock solution of AMG0347 (3.5 mg/ml), AMG 517 (3 mg/ml), and AMG8163 (6.7 mg/ml) were stored at -80°C . On the day of an experiment, the stock of interest was diluted with saline to achieve a 50% ethanol concentration (working solution). In thermophysiological experiments, these working solutions were infused into unanesthetized rats i.v. at a volume rate of 167 $\mu\text{l}/\text{kg}/\text{min}$ for 2 min to deliver the antagonist at a total dose of 50 $\mu\text{g}/\text{kg}$ (AMG0347), 100 $\mu\text{g}/\text{kg}$ (AMG 517), or 70 $\mu\text{g}/\text{kg}$ (AMG8163). For each antagonist, this total dose was previously characterized as the minimal dose causing the maximal hyperthermic effect [4,37]. In electrophysiological experiments, AMG0347 was delivered to anesthetized rats at a final dose of 500 $\mu\text{g}/\text{kg}$. The higher dose of AMG0347 was needed for these experiments, because anesthesia itself attenuates the hyperthermic response to TRPV1 antagonists [39].

RTX, a highly potent TRPV1 agonist [2,19], was purchased from Sigma-Aldrich. An ethanolic stock solution of RTX (200 $\mu\text{g}/\text{ml}$) was prepared, aliquoted, and stored at -80°C . On the day of the experiment, the stock was diluted with saline to achieve a final RTX concentration of 0.1, 2, or 20 $\mu\text{g}/\text{ml}$ at a final ethanol concentration of 10%. To induce abdominal desensitization of TRPV1 channels, the working solution of RTX (20 $\mu\text{g}/\text{ml}$) was injected i.p. as a bolus (1 ml/kg), using a 26 ga needle. In the writhing test, RTX (0.1 $\mu\text{g}/\text{ml}$) was injected i.p. as a bolus (1 ml/kg). A drop of RTX (2 $\mu\text{g}/\text{ml}$) was applied to the cornea in the

eye-wiping test at St. Joseph's Hospital and Medical Center.

Capsaicin was obtained from Reanal. A stock solution of capsaicin (10 mg/ml) was prepared containing 10% ethanol and 10% Tween-80 in saline. On the day of the experiment, the stock solution was diluted with saline to make a 10 µg/ml working solution. This working solution (or the vehicle) was dropped in the eye of the rats in the eye-wiping test at the University of Pecs. In blood-perfusion measurements, capsaicin was dissolved in saline containing 10% ethanol and 5% Tween-80 at a concentration of 6 mg/ml on the day of the experiment. This solution (or its vehicle) was injected as a bolus (50 µl) into the abdominal muscle to deliver capsaicin at a dose of 300 µg.

CL316243, a highly selective agonist of the β_3 -adrenergic receptor [40] (the "metabolic" receptor in BAT [41]), was purchased from Tocris. An aqueous stock solution of the drug (15 mg/ml) was prepared, which was further diluted with saline on the day of the experiment to contain CL316243 at 3 mg/ml. This working solution was infused i.v. at a rate of 333 µl/kg/min over 1 min to deliver 1 mg/kg of CL316243.

Immunohistochemistry

Procedure for immunohistochemical staining for c-Fos followed our previous study [42]. The brain tissues were cut into 30-µm-thick frontal sections on a freezing microtome. The sections were incubated overnight with anti-Fos rabbit serum (1:10,000; Ab-5; Oncogene) and then for 1 h with biotinylated donkey antibody to rabbit IgG (10 µg/ml; Chemicon). The sections were further incubated for 1 h with avidin-biotinylated peroxidase complex (ABC-Elite; 1:50; Vector). Bound peroxidase was visualized by incubating the sections with a solution containing 0.02% 3,3'-diaminobenzidine tetrahydrochloride (Sigma), 0.001% hydrogen peroxide, and 50 mM Tris-HCl (pH 7.6).

Anatomy and cell counting. The anatomical nomenclature and nuclear boundaries followed the brain atlas of Paxinos and Watson [43], except for the rRPa, which was defined as a part rostral to the rostral pole of the inferior olivary complex and has been shown to harbor a major population of sympathetic premotor neurons for thermoregulation

[42,44]. The c-Fos-immunoreactive cells were counted in the rRPa in every sixth 30-µm-thick frontal section with the ImageJ software (NIH) by a single examiner, who was blinded to the treatment of the rats.

Data processing and analysis

The rate of VO_2 was calculated by comparing the oxygen fraction in the air exiting the chamber occupied by a rat (F_{rat}) to the oxygen fraction in the air exiting an empty chamber (F_0). The following formula was used:

$$VO_2 = \frac{A(F_0 - F_{rat})}{M - F_0M(1 + Q)}$$

where A is air flow, Q is the respiratory quotient (considered to be 0.71), and M is the animal mass [4,32,37].

Thermoregulatory responses, blood-flow intensities, tail flick latencies, and numbers of c-Fos-positive cells were compared by one-way or two-way ANOVA followed by Fisher's *post hoc* test, as appropriate. To compare writhing and eye-wiping responses between groups, the Mann-Whitney U test was used. All other data collected as single-point measurements (stomach mass, blood corticosterone level) were compared between the treatment groups by Student's t test. Statistical analyses were performed using Statistica AX'99 (StatSoft) and Sigmaplot 11.0 (Systat Software). Data are presented as the mean \pm SE.

Results

Experiment 1. Intact functionality of RTX-sensitive abdominal nerves is required for the development of TRPV1 antagonist-induced hyperthermia

To verify that TRPV1 antagonists cause hyperthermia through an abdominal site of action, we induced localized abdominal desensitization of TRPV1 channels with a low dose of RTX (20 µg/kg, i.p.), as in earlier studies in rats [4–6,31]. The thermoregulatory response to three TRPV1 antagonists (AMG0347, AMG 517, and AMG8163) was studied in the desensitized rats. Consistent with our earlier study [4], administration of AMG0347 (50 µg/kg, i.v.) to

sham-desensitized rats caused a pronounced rise in their deep T_b , whereas the same dose of AMG0347 failed to cause any change in T_b when administered to RTX-pretreated rats

(ANOVA, $F_{(60,549)} = 2.4$, $p < 1.0 \times 10^{-3}$) (Figure 1a). Next, we tested whether desensitization of the abdominal TRPV1 channels can abolish the hyperthermic responses to AMG 517 and

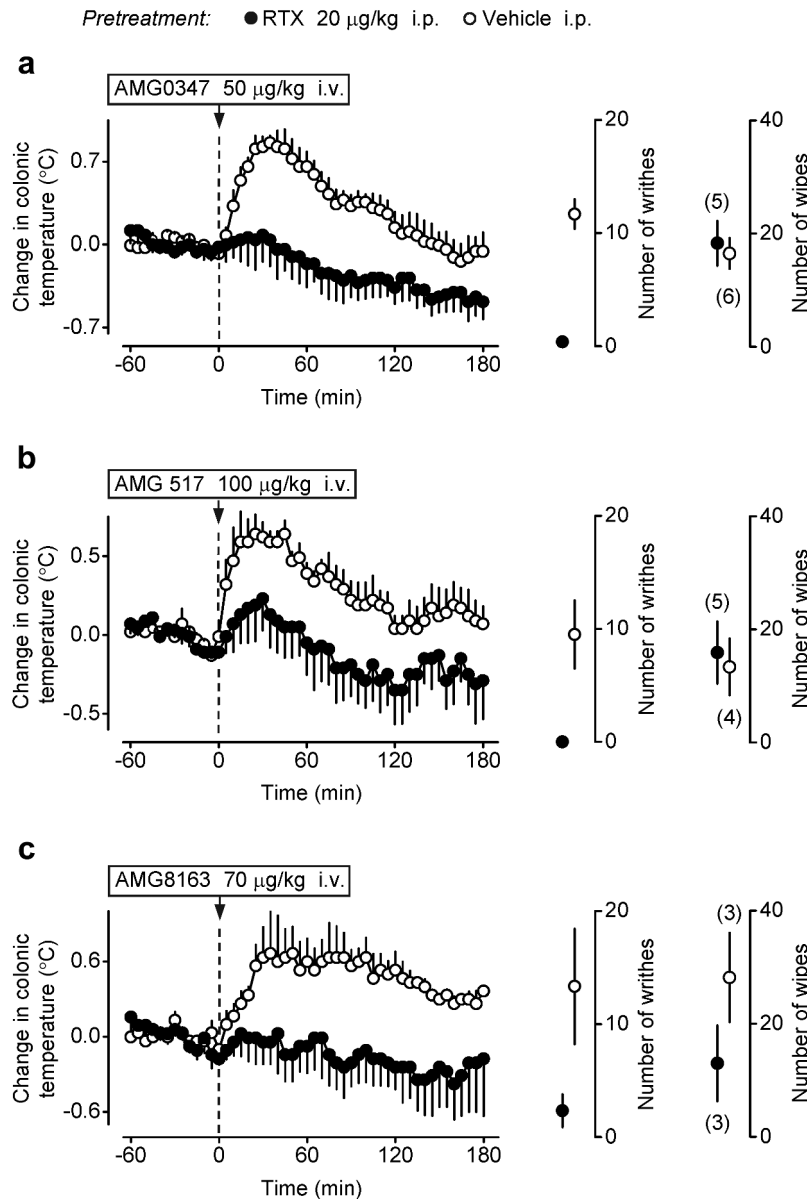


Figure 1. TRPV1 antagonist-induced hyperthermia is abolished in rats with localized abdominal desensitization of TRPV1 channels with a low dose of i.p. RTX. Rats pretreated with vehicle (sham-desensitized) responded to the i.v. administration of AMG0347 (a), AMG 517 (b), or AMG8163 (c) with a pronounced T_b rise, whereas no hyperthermic response occurred in rats desensitized with i.p. RTX (20 $\mu\text{g}/\text{kg}$). Doses of the TRPV1 antagonists used are indicated. In each panel, data plotted to the right of the temperature curves show two responses of the same sham-desensitized and desensitized rats that were used to study the hyperthermic effect of the corresponding TRPV1 antagonist: 1) the number of writhes (during 10 min) induced by the i.p. administration of RTX (0.1 $\mu\text{g}/\text{kg}$) and 2) the number of eye-wiping movements (during 5 min) induced by the epicorneal application of RTX solution (2 $\mu\text{g}/\text{ml}$, 20 μl). In all panels (a-c), vehicle-pretreated rats had a strong writhing reflex, whereas this reflex was absent in rats pretreated with i.p. RTX, thus confirming successful desensitization of TRPV1 channels in the peritoneal cavity by the latter pretreatment. In contrast, there was no difference between RTX-desensitized and sham-desensitized animals in the eye-wiping test, indicating that extra-abdominal TRPV1 channels were not affected by the i.p. RTX pretreatment. Here and in Figures 2–4, numbers in parentheses are the numbers of animals in the corresponding groups, and the data are presented as the mean \pm SE.

AMG8163. When administered to vehicle-pretreated rats, AMG 517 (100 $\mu\text{g}/\text{kg}$, i.v.) caused a marked increase in deep T_b , but in RTX-pretreated rats the same dose of AMG 517 did not cause any significant change in T_b (Figure 1b). The effect of AMG 517 was significantly different on T_b between the RTX- and vehicle-pretreated groups (ANOVA, $F_{(1,427)} = 148.5$, $p < 1.0 \times 10^{-3}$). The T_b of the vehicle-pretreated rats was higher than in RTX-pretreated rats at 15–110 min after AMG 517 administration (Fisher LSD test, $p < 5.0 \times 10^{-2}$). Similarly to AMG0347 and AMG 517, the hyperthermic response to AMG8163 (70 $\mu\text{g}/\text{kg}$, i.v.) was abolished in the desensitized rats compared to sham-desensitized rats (ANOVA, $F_{(1,244)} = 173.9$, $p < 1.0 \times 10^{-3}$) (Figure 1c). In the sham-desensitized rats, we did not observe any meaningful difference in the dynamics of the hyperthermic response among the three TRPV1 antagonists, so we used AMG0347 in the rest of the study.

To confirm the desensitization of intra-abdominal TRPV1 channels, we studied the writhing response to RTX (0.1 $\mu\text{g}/\text{kg}$, i.p.). This response was almost completely ablated in RTX-desensitized rats compared (by Mann-Whitney U test) to sham-desensitized rats in all three TRPV1 antagonist treatment groups: AMG0347 ($p = 6.2 \times 10^{-3}$), AMG 517 ($p = 1.4 \times 10^{-2}$), and AMG8163 ($p = 4.9 \times 10^{-2}$) (Figure 1). There was no difference between desensitized and sham-desensitized animals in the eye-wiping test in any of the three treatment groups.

These results show clearly that the development of TRPV1 antagonist-induced hyperthermia requires the functional integrity of RTX-sensitive nerves in the abdomen.

Experiment 2. TRPV1 antagonist-induced hyperthermia does not require the integrity of the abdominal vagal trunks

To test whether the abdominal vagus is involved in the development of TRPV1 antagonist-induced hyperthermia, we studied thermoregulatory responses to i.v. AMG0347 in rats with bilateral subdiaphragmatic truncal vagotomy. The vagotomized and the sham-vagotomized rats both responded to AMG0347

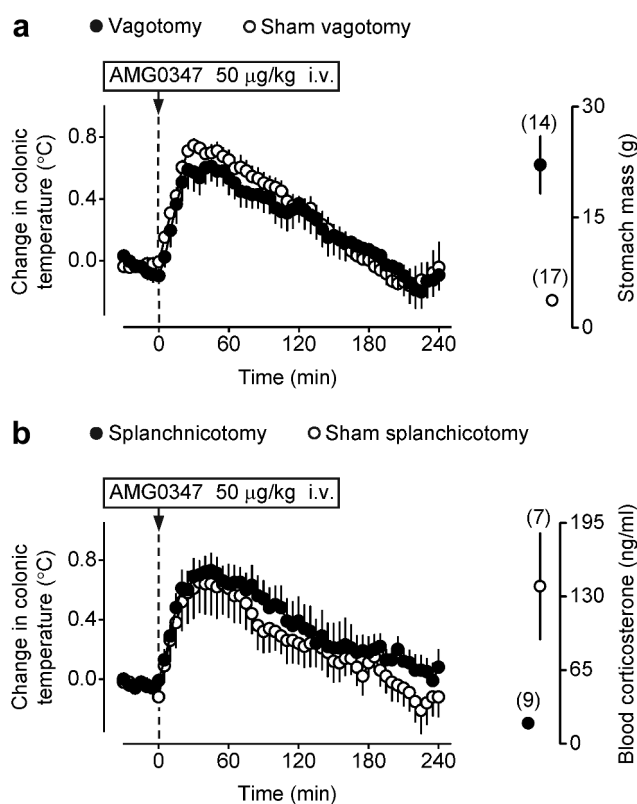


Figure 2. TRPV1 antagonist-induced hyperthermia is not affected by either total subdiaphragmatic truncal vagotomy or bilateral transection of the greater splanchnic nerve. **(a)** Sham-vagotomized rats and rats with total subdiaphragmatic truncal vagotomy responded to the i.v. administration of AMG0347 (dose indicated) with nearly identical rises in T_b . Confirming the effectiveness of vagotomy, the stomach mass was drastically increased in vagotomized rats, as compared to sham-vagotomized controls (right portion of panel **a**). **(b)** Sham-splanchnicotomized rats and rats with bilateral transection of the greater splanchnic nerve responded to the i.v. administration of AMG0347 with similar T_b rises. Confirming the effectiveness of splanchnicotomy, the blood corticosterone response to 48-h water deprivation was dampened in splanchnicotomized rats, as compared to sham-splanchnicotomized controls (right portion of panel **b**).

(50 $\mu\text{g}/\text{kg}$, i.v.) with a $\sim 0.7^\circ\text{C}$ increase in deep T_b , and there was no difference between the groups (Figure 2a). At the end of the recording period, the rats were euthanized with pentobarbital sodium (100 mg/kg i.v.), and then their stomachs were excised and weighed (together with stomach contents). Confirming the effectiveness of the vagotomy [23,26,45], the stomach mass was significantly ($t_{(29)} = -5.4$, $p = 8.0 \times 10^{-6}$) higher in the vagotomized rats than in the sham-vagotomized rats (Figure 2a).

These results suggest that TRPV1 antagonist-induced hyperthermia does not require the integrity of the abdominal vagi.

Experiment 3. TRPV1 antagonist-induced hyperthermia does not require the integrity of the greater splanchnic nerves

To test whether the greater splanchnic nerves mediate TRPV1 antagonist-induced hyperthermia, we studied thermoregulatory responses to i.v. AMG0347 in rats subjected to bilateral transection of the greater splanchnic nerve. When we infused AMG0347 to splanchnicotomized and sham-splanchnicotomized rats, both groups responded to the drug with marked ($\sim 0.7^\circ\text{C}$) hyperthermia, which was not different between the groups (Figure 2b). To confirm the efficacy of splanchnicotomy, we studied the stress response of the rats by detecting their blood corticosterone levels after water deprivation [29]. We found that splanchnicotomized rats responded to the stressful stimulus with a significantly attenuated increase in blood corticosterone compared to the sham-splanchnicotomized controls (19 ± 4 vs 139 ± 46 ng/ml, respectively; $t_{(13)} = 2.9$, $p = 1.0 \times 10^{-2}$) (Figure 2b).

These results suggest that the greater splanchnic nerve does not participate in the development of TRPV1 antagonist-induced hyperthermia, at least not as obligatory sole or major conductor.

Experiment 4. The integrity of the DLF of the spinal cord is required for the development of TRPV1 antagonist-induced hyperthermia

Next, we tested whether spinal pathways running within the DLF are required for the hyperthermic response to a TRPV1 antagonist. For that, we performed bilateral dorsolateral funiculotomy or sham funiculotomy and treated the rats with AMG0347 (Figure 3a). We found that in animals with incomplete or sham lesions, AMG0347 caused an elevation of deep T_b by $\sim 0.6^\circ\text{C}$, which started at 5–10 min post-administration and peaked at 25–55 min. In contrast with sham dorsolateral funiculotomy, the hyperthermic response of rats to AMG0347 was markedly attenuated after

complete dorsolateral funiculotomy (ANOVA, $F_{(60,854)} = 2.0$, $p = 1.8 \times 10^{-5}$).

The completeness of the lesion was confirmed in each animal functionally with the tail flick test (Figure 3a) and morphologically with histology (Figure 3b). We observed a significant prolongation of the tail flick latency in the complete (12 ± 2 s; Fisher LSD test, $p = 1.3 \times 10^{-2}$) and incomplete dorsolateral funiculotomy groups (10 ± 1 s; Fisher LSD test, $p = 1.9 \times 10^{-2}$) compared to the sham-lesioned rats (6 ± 1 s).

Importantly, some rats with complete dorsolateral funiculotomy showed sporadic, sharp T_b rises in the course of their response to AMG0347 (Figure 3c), thus demonstrating full competence of their cold-defense thermoeffectors. Furthermore, one group of rats was selected from the studied population and tested with the β_3 -adrenergic receptor agonist, CL316243, to confirm that rats with complete dorsolateral funiculotomy are capable of elevating their deep T_b to the same extent as rats in the incomplete DLF lesioning and sham funiculotomy groups. Among these randomly selected rats, two animals were histologically confirmed to have complete lesions and both of them responded to CL316243 with a marked elevation of VO_2 and T_b , which were undistinguishable from the metabolic and thermal responses of incomplete- and sham-lesioned rats (Figure 3c).

These data show that the integrity of the DLF is required for the development of TRPV1 antagonist-induced hyperthermia. Because rats with reasonably complete bilateral transection of the DLF were fully capable of increasing thermogenesis, the attenuation of TRPV1 antagonist-induced hyperthermia is unlikely to be caused by thermoeffector insufficiency.

Experiment 5. Capsaicin-induced vascular responses in the abdominal-wall muscles are absent in rats pretreated with i.p. RTX

The experiments reported above indicate that the mechanisms of TRPV1 antagonist-induced hyperthermia involve an action on TRPV1-bearing sensory nerves in the abdomen, and that signals conveyed by these nerves reach the brain not through the vagi, but via the spinal cord; yet they

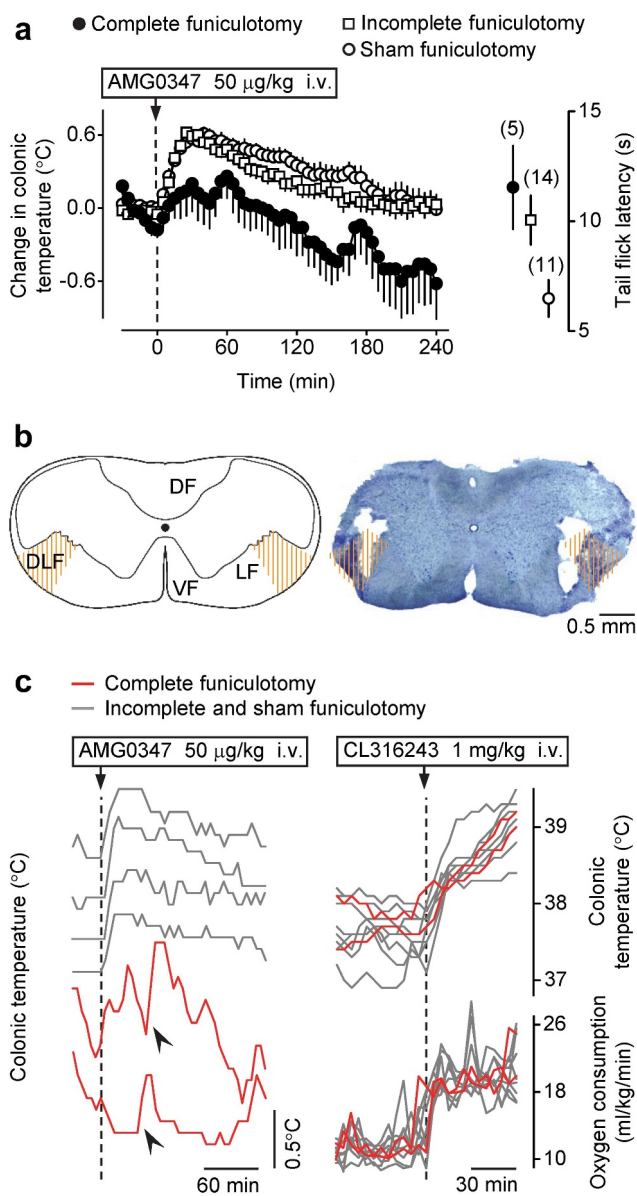


Figure 3. TRPV1 antagonist-induced hyperthermia is attenuated by bilateral cervical transection of the DLF of the spinal cord. **(a)** Rats with complete bilateral cervical dorsolateral funiculotomy responded to i.v. AMG0347 (dose indicated) with a much smaller T_b rise than either sham-funiculotomized controls or rats with incomplete cervical dorsolateral funiculotomy. Data plotted in the right part of panel **a** show that the tail-flick response to noxious (-18° C) cold was delayed in rats with complete or incomplete dorsolateral funiculotomy, as compared to sham-funiculotomized controls. **(b)** A schematic of a transversal C1 spinal section from Paxinos and Watson [46] and a representative bright-field photomicrograph of a C1 section with a complete bilateral lesion of the DLF from a rat used in this study (50 μ m, cresyl violet). The targeted lesion area on each side of the spinal cord (DLF) is hatched with orange lines; only rats having a lesion covering $>50\%$ of the targeted area on each side were considered having “complete” funiculotomy. DF, LF, VF – dorsal, lateral, or ventral funiculus, respectively. **(c)** Rats with complete dorsolateral funiculotomy did not respond with hyperthermia to a TRPV1 antagonist but mounted robust thermogenic and hyperthermic responses to a β_3 agonist. On the left, individual T_b curves show that the hyperthermic response to i.v. AMG0347 (dose indicated) occurred in rats with an intact or partially lesioned DLF but not in rats with complete dorsolateral funiculotomy. Nevertheless, even rats with complete funiculotomy were capable of sporadically developing sharp rises in deep T_b (indicated by arrowheads). On the right, individual deep T_b and $\dot{V}O_2$ curves show that the hyperthermic and thermogenic responses to i.v. CL316243 (β_3 -adrenergic receptor agonist; dose indicated) did not differ between rats with sham, incomplete, or complete dorsolateral funiculotomy.

do not travel through the greater splanchnic nerves. We hypothesized that such spinally mediated (but not splanchnic-mediated) signals

may originate from TRPV1 channels in abdominal skeletal muscles. If this hypothesis is true, the desensitization occurring after the i.p.

administration of a low dose of RTX (*Experiment 1*), should involve TRPV1-expressing afferents in the abdominal-wall muscles. To test if this is the case, we measured the topical capsaicin-induced changes in blood perfusion of the external oblique abdominal muscle in RTX-desensitized and sham-desensitized rats. The local i.m. (between the external and internal oblique abdominal muscle) administration of capsaicin caused a marked reduction in the muscular blood flow in sham-desensitized rats, however the same dose of capsaicin had no effect in RTX-desensitized rats (**Figure 4a-b**). The effect of capsaicin on blood flow was significantly different between the RTX- and vehicle-pretreated groups (ANOVA, $F_{(1,518)} = 22.5$, $p < 1.0 \times 10^{-3}$). The blood flow in the vehicle-pretreated rats was lower than in RTX-pretreated rats at 30–100 s after capsaicin administration (Fisher LSD test, $p < 5.0 \times 10^{-2}$). The i.m. injection of this dose of capsaicin did not affect the systolic carotid blood pressure (**Figure 4a**).

As in the thermophysiological experiments, the writhing response to RTX was almost absent in RTX-desensitized rats compared to sham-desensitized rats (Mann-Whitney U test, $p < 1.0 \times 10^{-3}$) (**Figure 4a**), whereas there was no difference between the two pretreatment groups in the eye-wiping test.

These data suggest that the attenuation of hyperthermic responses to TRPV1 antagonists observed in *Experiment 1* may be explained by desensitization of afferent TRPV1-expressing nerves servicing abdominal muscles.

Experiment 6. Signals from abdominal TRPV1 channels impinge on the established thermoeffector pathways

Since the TRPV1 antagonist-induced elevation of deep T_b is brought about by the activation of cold-defense effectors [4,37], and the hyperthermic response to AMG0347 involves spinal afferents, we hypothesized that AMG0347 increases deep T_b by blocking a TRPV1 channel-activated afferent pathway that normally suppresses the activity of neurons at some point within the brain pathway driving autonomic cold defenses in response to skin cooling [35]. To test this hypothesis, we used electrophysiological techniques in

combination with a chemical inactivation of localized neuronal populations in the brain. We found that antagonism of TRPV1 channels with i.v. AMG0347 produced an increase in BAT SNA and in T_{BAT} (reflecting an increase in BAT thermogenesis) (**Figure 5a**). The increase in BAT SNA evoked by AMG0347 was reversed by muscimol-induced inhibition of neuronal activity in the LPB (**Figure 5a**), which is located in the thermosensory afferent pathway between dorsal horn and preoptic area, and it is necessary for sympathetic activation of BAT in response to skin cooling [35,47]. The AMG0347-induced response in BAT SNA was also abolished by inhibition of neuronal activity in the rRPa with glycine (**Figure 5a**), which is the site of sympathetic premotor neurons controlling BAT sympathetic outflow [47]. We also measured the expression of the inducible transcription factor c-Fos, a marker of neuronal activation [48], in the rRPa (**Figure 5b**). In agreement with our previous report [44], we found that 1 h cold exposure (4°C) increased the c-Fos immunoreactivity expression in the rRPa (Fisher LSD test, $p = 4.0 \times 10^{-4}$). Similar to cold exposure, a significant increase in the number of c-Fos-positive neurons was detected following i.v. infusion of AMG0347 (Fisher LSD test, $p = 2.0 \times 10^{-2}$), as compared to controls.

These data show that AMG0347 stimulates BAT thermogenesis via the same autonomic thermoeffector pathway as skin cooling.

Discussion

Neural pathway of TRPV1 antagonist-induced hyperthermia

In the present study, we showed that hyperthermic responses to three TRPV1 antagonists, *viz.*, AMG0347, AMG 517, and AMG8163, did not occur in rats pretreated with a low i.p. dose of RTX (20 µg/kg) (*Experiment 1*, **Figure 6**). This RTX pretreatment is known to desensitize the sensory nerves in the abdomen, but not in the thoracic viscera, brain, cornea, or skin [4,5]. The localized abdominal TRPV1 desensitization was previously shown to attenuate hyperthermic responses to AMG0347 [4] and to yet another TRPV1 antagonist, A889425 [6]. The fact that this phenomenon has now been demonstrated for

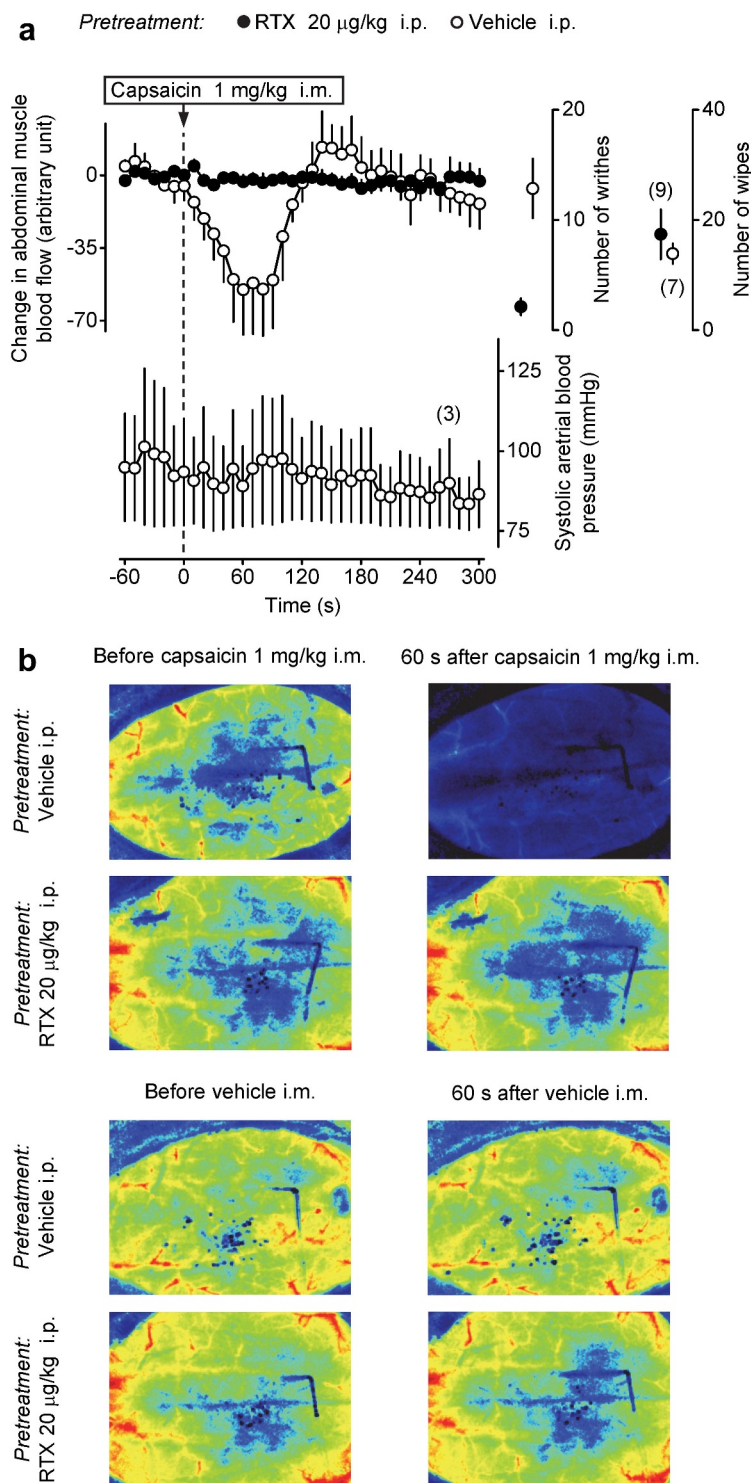


Figure 4. The hypoperfusion response in the external oblique abdominal muscle to topical application of a TRPV1 agonist is abolished in rats desensitized with a low dose of i.p. RTX. (**a**) The upper curves in the left portion show that a rapid and profound decrease in blood flow in the external oblique abdominal muscle in response to topical administration of capsaicin (dose indicated) occurs in rats pretreated with vehicle (sham-desensitized) but not in rats pretreated with i.p. RTX (20 $\mu\text{g}/\text{kg}$) to induce localized abdominal TRPV1 desensitization. The lower curve shows that, in three randomly selected sham-desensitized rats, i.m. capsaicin caused no changes in the carotid blood pressure. Data plotted in the right portion of panel **a** show two responses of the same sham-desensitized and desensitized rats that were used in the perfusion experiment: 1) the number of writhes (during 10 min) induced by the i.p. administration of RTX (0.1 $\mu\text{g}/\text{kg}$) and 2) the number of eye-wiping movements (during 1 min) induced by the epicorneal application of capsaicin solution (10 $\mu\text{g}/\text{ml}$, 40 μl). Vehicle-pretreated rats had a strong writhing reflex, whereas this reflex was absent in rats pretreated with i.p. RTX, thus confirming successful desensitization of TRPV1 channels in the peritoneal cavity by the

four compounds firmly establishes the abdomen as the site where TRPV1 antagonists act on TRPV1 channels to trigger hyperthermia. It has also been established in experiments with selective elimination of TRPV1 expression in sensory neurons that TRPV1 antagonists trigger hyperthermia by acting on TRPV1 channels on nerve afferents [7].

Next, we studied how the signals that originate from TRPV1 channels on afferent nerves somewhere in the abdomen are conveyed to the brain. The abdominal viscera are innervated by the several nerves, including the vagus, the largest nerve in the body, which is predominantly sensory, with its afferent fibers expressing TRPV1 [13,49,50]. In *Experiment 2*, we excluded the vagal mediation of TRPV1 antagonist-induced hyperthermia by showing that total truncal subdiaphragmatic vagotomy did not affect the T_b rise caused by i.v. AMG0347, even though the effectiveness of vagotomy was confirmed functionally, by the greatly increased stomach mass after the surgery.

The abdominal viscera are also serviced by the greater, lesser, least, lumbar, and pelvic splanchnic nerves [8,51]. The splanchnic nerves express TRPV1 channels [11,12], and the TRPV1 protein expression levels are generally higher on splanchnic afferents than on vagal ones [12,13]. However, in our *Experiment 3*, bilateral transection of the greater splanchnic nerve did not affect AMG0347-induced hyperthermia, even though the effectiveness of splanchnicotomy was verified functionally, by the blockade of stress-induced corticosterone production by the adrenals after splanchnicotomy.

In contrast to vagotomy and splanchnicotomy, bilateral transection of the dorsal portion of the lateral funiculus at the C1 level attenuated the hyperthermic response to i.v. AMG0347 (*Experiment 4*), thereby suggesting that signals that originate from abdominal TRPV1 channels and trigger the hyperthermic response ascend through the spinal cord. The spinal mediation of the hyperthermic response to TRPV1 antagonists

is also confirmed by the data showing that mice with TRPV1 desensitization caused by intrathecal capsaicin did not respond with hyperthermia to AMG 517 [7]. In several animal species, noxious and various innocuous signals, both visceral and somatic, travel in the lateral funiculus, within the spinothalamic and spinoparabrachial tracts [35,52,53]. These signals include temperature signals from the trunk and extremities [35,54–56]. Lesions of the DLF in the cervical spinal cord were reported to result in thermosensory deficiencies in cats [57,58] and attenuate cold-avoidance behavioral responses in rats [30].

Since bilateral transection of the greater splanchnic nerve did not block the hyperthermic response to AMG0347 (*Experiment 3*), we know that the spinally transmitted signals that drive TRPV1 antagonist-induced hyperthermia do not reach the spinal cord through the greater splanchnic. *A priori*, the lesser, least, lumbar, and pelvic splanchnic nerves may be involved, but all of them are much smaller than the greater splanchnic nerve and service the relatively small amount of tissue in various organs at the bottom of the abdominal cavity [9,10]. Furthermore, among the splanchnic nerves, both the level of TRPV1 expression and the percentage of capsaicin-sensitive fibers generally decrease in the caudal direction, from the greater nerve to the pelvic one [14].

In view of the above, the alternative hypothesis, *i.e.*, that the signals of interest travel to the spinal cord through the somatic afferents of the abdominal wall, a massive assemblage of skeletal muscles, is more attractive. These somatic afferents are predominantly metabosensitive C-fibers [59], which ascend through the spinal cord within the DLF [60]. During strenuous physical exercise, contracting skeletal muscles produce metabolic acidosis and hyperthermia, both of which activate TRPV1 channels [61]. Among other TRPV1-mediated effects of the decreased interstitial pH in muscle is the modulation of the pressor reflex [62].

latter pretreatment. In contrast, there was no difference between sham-desensitized and RTX-desensitized rats in the eye-wiping test, indicating that extra-abdominal, at least corneal, TRPV1 channels were not affected by the i.p. RTX pretreatment. **(b)** Individual speckle photographs of the abdominal wall represent perfusion responses to capsaicin and vehicle of sham-desensitized and i.p. RTX-desensitized rats. For each rat and each treatment, a representative baseline (before-treatment) image is shown on the left, and a representative after-treatment (at 60 s after the i.m. administration of vehicle or capsaicin) is shown on the right.

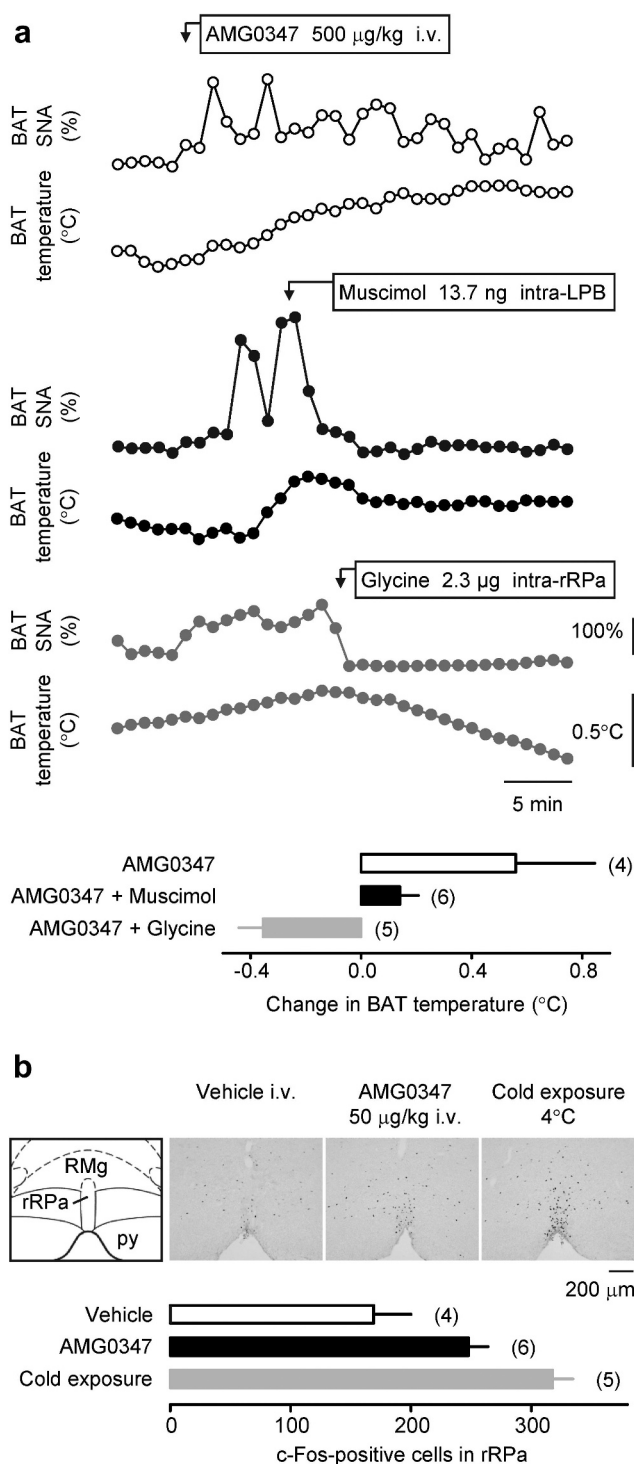


Figure 5. The signals driving TRPV1 antagonist-induced hyperthermia travel through the brain via the established neural pathways that control autonomic thermoeffector. **(a)** Individual curves demonstrate that the i.v. administration of AMG0347 (the dose is indicated) caused relatively long-lasting (the time-scale bar is shown) increases in BAT SNA and T_{BAT} in an anesthetized rat (top panel). Rats represented in the middle and lower panels received the same i.v. administration of AMG0347 (not shown) as the rat represented in the top panel and 7–12 min later received either an injection of muscimol (dose indicated) into the LPB (middle panel) or an injection of glycine (dose indicated) into the rRPa (lower panel). Either treatment rapidly decreased both BAT SNA and T_{BAT} . The bar graph at the bottom of panel **a** shows that the mean T_{BAT} increase induced by i.v. AMG0347 was markedly attenuated by either intra-LPB injection of muscimol or intra-rRPa injection of glycine. **(b)** AMG0347 increased c-Fos expression in the rRPa. Main structures of the rRPa-containing brain area are outlined in the schematic from Paxinos and Watson [43] on the left; py – pyramidal tract; RMg – raphe magnus nucleus. To the right of the schematic, representative photomicrographs of the same brain area show c-Fos-positive neurons. The sections were obtained from rats treated with vehicle or i.v. AMG0347 (dose indicated) in a near-thermoneutral environment, or exposed to severe cold (ambient temperature is indicated; positive control). The bar graph at the bottom of panel **b** shows that the number of c-Fos-positive cells in the rRPa was higher in rats treated with i.v. AMG0347 at thermoneutrality or exposed to cold, as compared to rats injected with vehicle at thermoneutrality.

If the abdominal-wall muscles do represent the site of the hyperthermic action of TRPV1 antagonists, then the desensitization caused by the i.p. administration of a low dose of RTX in *Experiment 1* of this study and in the earlier studies [4,6] should have spread into the abdominal wall to include TRPV1-expressing afferents in skeletal muscles of the trunk. Hence, we studied whether a capsaicin-evoked reflex was attenuated in the external oblique abdominal muscle of RTX-desensitized rats (*Experiment 5*). We found that, in control (vehicle-pretreated) rats, topical (in the abdominal wall) administration of capsaicin markedly decreased the blood perfusion in the adjacent external oblique muscle by causing arteriole vasoconstriction. While TRPV1 channels expressed in vascular smooth muscle cells play an important role in mediating the constriction of resistance arteries [63], TRPV1 channels on perivascular nerves, including on C-fibers, are also involved [64,65]. In contrast with vehicle-pretreated rats, the capsaicin-induced decrease in perfusion was completely abolished in rats pretreated with a low dose of i.p. RTX. This finding shows that the localized abdominal desensitization of afferent nerves that results in the attenuation of TRPV1 antagonist-induced hyperthermia involves TRPV1 channels in the abdominal skeletal muscles. Taken together with all other results of the present study (Figure 6), this finding leads us to the conclusion that TRPV1 antagonists are likely to trigger the hyperthermic effect by acting on TRPV1 channels in trunk muscles.

We also questioned whether the hyperthermic response to TRPV1 antagonists involves the known brain circuitry mediating autonomic thermoeffector responses to skin cooling [47]. In *Experiment 6*, we first tested the involvement of the LPB, which receives cutaneous cold and warmth signals from primary sensory neurons [35]. We showed that intra-LPB administration of muscimol (to inhibit local neuronal activity) blocked BAT thermogenesis and hyperthermia induced by the i.v. administration of AMG0347. We also examined whether neurons in the rRPa, which contains premotor neurons for the thermogenic and vasomotor thermoeffectors, are required for the TRPV1 antagonist-induced hyperthermia. We showed that the i.v. administration of AMG0347 elicited a strong increase in the number of c-Fos-positive cells

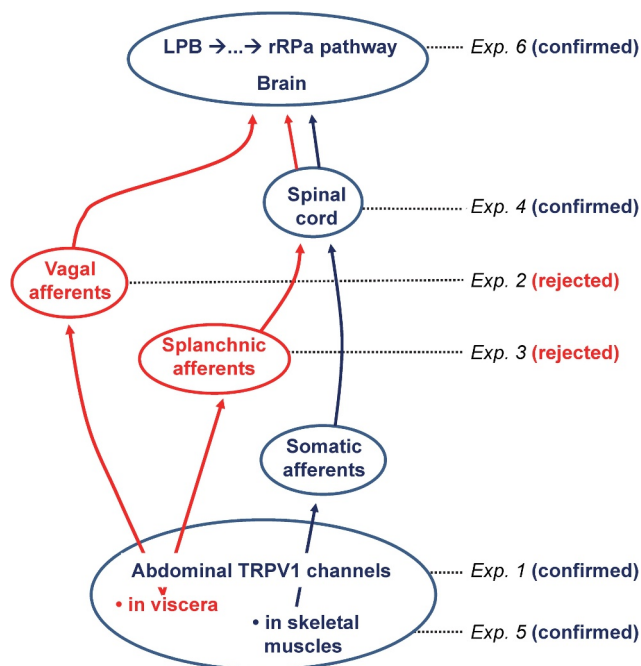


Figure 6. In rats, the proposed neural pathway of TRPV1 antagonist-induced hyperthermia starts with TRPV1 channels in skeletal muscles of the trunk, goes through the DLF of the spinal cord, and, at an unknown spinal or brainstem site, joins the established LPB-rRPa pathway that drives thermogenesis. Alternative pathways rejected by the present study are shown in red. For each experiment of the present study, the tested pathway, or the tested portion of a pathway, is indicated.

in the rRPa, whereas intra-rRPa administration of glycine, an inhibitory amino acid neurotransmitter, blocked the activation of BAT thermogenesis and T_b rise evoked by AMG0347. These results indicate that there is a population of neurons in the LPB that is required for the hyperthermic response to i.v. AMG0347, and that rRPa neurons are also necessary for the hyperthermic response to AMG0347. These results are consistent with a model in which the central projections of the TRPV1-expressing abdominal afferents impinge on the brain circuits driving autonomic cold defenses (Figure 6). In this regard, it seems most likely that the site(s) at which the TRPV1-expressing afferents interact with the cold-defense pathway is either the spinal dorsal horn or LPB.

Significance

By integrating the results of the present study with our previous work on the mechanisms of the hyperthermic effect of TRPV1 antagonists [4,37], we propose that, in rats, these pharmacological

compounds act on TRPV1 channels on afferents innervating trunk skeletal muscles and block tonic (by protons) activation of these channels to disinhibit BAT thermogenesis and skin vasoconstriction. The neural pathway for this effect ascends through the spinal cord within the DLF and impinges on the LPB-rRPa pathway for autonomic cold defenses. This neural pathway comprises the substrate of the proposed acido-antithermogenic reflex, and possibly of the acido-antivasoconstrictor reflex as well [1]. These reflexes may play an important role in the regulation of deep T_b during physical activity [1,31], in line with the earlier proposal of TRPV1 activation improving exercise endurance [66]. Strenuous physical activity causes hyperthermia that limits performance [67] and can be deadly. Strenuous physical activity also causes metabolic acidosis, including marked acidemia [68], thus augmenting the activation of TRPV1 by protons in the massive trunk muscles that are rich with slow-twitch, type-1 muscle fibers and are involved in breathing [1]. The augmentation of TRPV1 activation further inhibits thermogenesis and skin vasoconstriction, thus preventing a further rise in T_b or bringing T_b down. Hence, the acido-antithermogenic and acido-antivasoconstrictor reflexes counteract the hyperthermia associated with physical activity. The novelty and significance of the present work are in outlining the neural pathways of the TRPV1-mediated acido-antithermogenic and acido-antivasoconstrictor reflexes.

Corollary

At least some effects of TRPV1 antagonists are age- or sex-specific ([69–71]; see ref. [1] for review). For example, the TRPV1 antagonist ABT-116 was reported to produce a stronger effect on locomotor activity in male than female dogs [72]. It has also been proposed that the differential exploitation for men and women (and younger and older) represents a development opportunity for drugs targeting TRPV1 and other TRP channels [73]. The present study suggests that the hyperthermic effect of TRPV1 antagonists originates in skeletal muscles. If what we found in rats applies to humans, then the substantially greater mass of skeletal muscles in men (as compared to

women) and younger adults (as compared to older) [74] may have implications for drug development: the hyperthermic side effect of TRPV1 antagonists may be speculated to be lesser in female and older patients. Many TRPV1 antagonists have been already tested in human clinical trials. Hence, the data needed to confirm or reject this hypothesis should be available, and a meta-analysis study may be warranted.

Abbreviations used

BAT: brown adipose tissue; C1, C2: first or second cervical vertebra, respectively; DLF: dorsolateral funiculus, the dorsal portion of the ventral funiculus; i.m.: intramuscular; i.p.: intraperitoneal(ly); i.v.: intravenous(ly); LPB: lateral parabrachial nucleus; rRPa: rostral raphe pallidus nucleus; RTX: resiniferatoxin; SNA: sympathetic nerve activity; T_b : body temperature; T_{BAT} : temperature of brown adipose tissue; TRP: transient receptor potential (channel); TRPV1: transient receptor potential cation channel subfamily V member 1; VO_2 : oxygen consumption.

Acknowledgments

The authors thank Rubing Xing for excellent histological support and Kata Bolcskei and Sondre Soderholm for assistance with blood-perfusion experiments.

Disclosure statement








A.A.R. is an officer and director of Catalina Pharma, Inc. and Zharko Pharma, Inc.; he has consulted for TRPV1 programs at several pharmaceutical companies, and his laboratory conducted paid research on TRPV1 for Amgen Inc., Abbott Laboratories, and AbbVie Inc.

Funding

This research has been supported by the National Institutes of Health (grants R01NS41233 to A.A.R. and R01NS40987 to S.F.M.), the National Research, Development and Innovation Office of Hungary (grant FK 138722 to A.G.), the Tempus Public Foundation (Hungarian State Eotvos Fellowship to A. G.), the Funding Program for Next Generation World-Leading Researchers from the Japan Society for the Promotion of Science (LS070 to K.N.), and the National Council for Scientific and Technological Development (Brazil) fellowship 200807/2008-0 (to S.P.W.).

ORCID

Andras Garami  <http://orcid.org/0000-0003-2493-0571>

Alexandre A. Steiner  <http://orcid.org/0000-0002-0802-4619>
 Samuel P. Wanner  <http://orcid.org/0000-0002-4659-1032>
 M. Camila Almeida  <http://orcid.org/0000-0002-2012-3169>
 Patrik Keringer  <http://orcid.org/0000-0002-9171-6834>
 Kazuhiro Nakamura  <http://orcid.org/0000-0002-6095-8996>
 Shaun F. Morrison  <http://orcid.org/0000-0002-8813-8359>
 Andrej A. Romanovsky  <http://orcid.org/0000-0003-3772-8575>

References

- [1] Garami A, Shimansky YP, Rumbus Z, et al. Hyperthermia induced by transient receptor potential vanilloid-1 (TRPV1) antagonists in human clinical trials: insights from mathematical modeling and meta-analysis. *Pharmacol Ther.* 2020;208:107474.
- [2] Romanovsky AA, Almeida MC, Garami A, et al. The transient receptor potential vanilloid-1 channel in thermoregulation: a thermosensor it is not. *Pharmacol Rev.* 2009;61(3):228–261.
- [3] Gavva NR, Treanor JJ, Garami A, et al. Pharmacological blockade of the vanilloid receptor TRPV1 elicits marked hyperthermia in humans. *Pain.* 2008;136(1–2):202–210.
- [4] Steiner AA, Turek VF, Almeida MC, et al. Nonthermal activation of transient receptor potential vanilloid-1 channels in abdominal viscera tonically inhibits autonomic cold-defense effectors. *J Neurosci.* 2007;27(28):7459–7468.
- [5] Dogan MD, Patel S, Rudaya AY, et al. Lipopolysaccharide fever is initiated via a capsaicin-sensitive mechanism independent of the subtype-1 vanilloid receptor. *Br J Pharmacol.* 2004;143(8):1023–1032.
- [6] McGaraughty S, Segreti JA, Fryer RM, et al. Antagonism of TRPV1 receptors indirectly modulates activity of thermoregulatory neurons in the medial preoptic area of rats. *Brain Res.* 2009;1268:58–67.
- [7] Yue WWS, Yuan L, Braz JM, et al. TRPV1 drugs alter core body temperature via central projections of primary afferent sensory neurons. *Elife* 2022; 11.
- [8] Berthoud HR, Blackshaw LA, Brookes SJ, et al. Neuroanatomy of extrinsic afferents supplying the gastrointestinal tract. *Neurogastroenterol Motil.* 2004;16(Suppl 1):28–33.
- [9] Alkatout I, Wedel T, Pape J, et al. Review: pelvic nerves - from anatomy and physiology to clinical applications. *Transl Neurosci.* 2021;12(1):362–378.
- [10] Loukas M, Klaassen Z, Merbs W, et al. A review of the thoracic splanchnic nerves and celiac ganglia. *Clin Anat.* 2010;23(5):512–522.
- [11] Holzer P. TRPV1 and the gut: from a tasty receptor for a painful vanilloid to a key player in hyperalgesia. *Eur J Pharmacol.* 2004;500(1–3):231–241.
- [12] Ward SM, Bayguinov J, Won KJ, et al. Distribution of the vanilloid receptor (VR1) in the gastrointestinal tract. *J Comp Neurol.* 2003;465(1):121–135.
- [13] Patterson LM, Zheng H, Ward SM, et al. Vanilloid receptor (VR1) expression in vagal afferent neurons innervating the gastrointestinal tract. *Cell Tissue Res.* 2003;311(3):277–287.
- [14] Brierley SM, Carter R, Jones W 3rd, et al. Differential chemosensory function and receptor expression of splanchnic and pelvic colonic afferents in mice. *J Physiol.* 2005;567(1):267–281.
- [15] Cavuoto P, McAinch AJ, Hatzinikolas G, et al. The expression of receptors for endocannabinoids in human and rodent skeletal muscle. *Biochem Biophys Res Commun.* 2007;364(1):105–110.
- [16] Lotteau S, Ducreux S, Romestaing C, et al. Characterization of functional TRPV1 channels in the sarcoplasmic reticulum of mouse skeletal muscle. *PLoS One.* 2013;8(3):e58673.
- [17] Onozawa K, Nakamura A, Tsutsumi S, et al. Tissue distribution of capsaicin receptor in the various organs of rats. *Proc Jpn Acad Ser B Phys Biol Sci.* 2000;76(5):68–72.
- [18] Xin H, Tanaka H, Yamaguchi M, et al. Vanilloid receptor expressed in the sarcoplasmic reticulum of rat skeletal muscle. *Biochem Biophys Res Commun.* 2005;332(3):756–762.
- [19] Szolcsanyi J. Effect of capsaicin on thermoregulation: An update with new aspects. *Temperature.* 2015;2(2):277–296. DOI:10.1080/23328940.2015.1048928.
- [20] Hoheisel U, Reinohl J, Unger T, et al. Acidic pH and capsaicin activate mechanosensitive group IV muscle receptors in the rat. *Pain.* 2004;110(1–2):149–157.
- [21] Kaufman MP, Iwamoto GA, Longhurst JC, et al. Effects of capsaicin and bradykinin on afferent fibers with ending in skeletal muscle. *Circ Res.* 1982;50(1):133–139.
- [22] Ootsuka Y, Blessing WW, Steiner AA, et al. Fever response to intravenous prostaglandin E2 is mediated by the brain but does not require afferent vagal signaling. *Am J Physiol Regul Integr Comp Physiol.* 2008;294(4):R1294–303.
- [23] Romanovsky AA, Kulchitsky VA, Simons CT, et al. Febrile responsiveness of vagotomized rats is suppressed even in the absence of malnutrition. *Am J Physiol.* 1997;273(2 Pt 2):R777–83.
- [24] Ellis H, Pryse-Davies J. Vagotomy in the rat. A study of its effects on stomach and small intestine. *Br J Exp Pathol.* 1967;48(2):135–141.
- [25] Sawchenko PE, Gold RM. Effects of gastric vs complete subdiaphragmatic vagotomy on hypothalamic hyperphagia and obesity. *Physiol Behav.* 1981;26(2):281–292.
- [26] Romanovsky AA, Ivanov AI, Lenczowski MJ, et al. Lipopolysaccharide transport from the peritoneal cavity to the blood: is it controlled by the vagus nerve? *Auton Neurosci.* 2000;85(1–3):133–140.

- [27] Dogan MD, Kulchitsky VA, Patel S, et al. Bilateral splanchnicotomy does not affect lipopolysaccharide-induced fever in rats. *Brain Res.* 2003;993(1–2):227–229.
- [28] Dijkstra I, Binnekade R, Tilders FJ. Diurnal variation in resting levels of corticosterone is not mediated by variation in adrenal responsiveness to adrenocorticotropin but involves splanchnic nerve integrity. *Endocrinology.* 1996;137(2):540–547.
- [29] Ulrich-Lai YM, Engeland WC. Adrenal splanchnic innervation modulates adrenal cortical responses to dehydration stress in rats. *Neuroendocrinology.* 2002;76(2):79–92.
- [30] Vizin RCL, Almeida MC, Soriano RN, et al. Selection of preferred thermal environment and cold-avoidance responses in rats rely on signals transduced by the dorso-lateral funiculus of the spinal cord. *Temperature.* 2023;10(1):121–135. DOI:10.1080/23328940.2023.2191378
- [31] Garami A, Pakai E, McDonald HA, et al. TRPV1 antagonists that cause hypothermia, instead of hyperthermia, in rodents: compounds' pharmacological profiles, in vivo targets, thermoeffector recruited and implications for drug development. *Acta Physiol (Oxf).* 2018;223(3):e13038.
- [32] Almeida MC, Hew-Butler T, Soriano RN, et al. Pharmacological blockade of the cold receptor TRPM8 attenuates autonomic and behavioral cold defenses and decreases deep body temperature. *J Neurosci.* 2012;32(6):2086–2099.
- [33] Romanovsky AA, Ivanov AI, Shimansky YP. Selected contribution: ambient temperature for experiments in rats: a new method for determining the zone of thermal neutrality. *J Appl Physiol.* 2002;92(6):2667–2679.
- [34] Olah E, Rumbus Z, Kormos V, et al. The hypothermic effect of hydrogen sulfide is mediated by the transient receptor potential ankyrin-1 channel in mice. *Pharmaceuticals (Basel).* 2021;14(10):992.
- [35] Nakamura K, Morrison SF. A thermosensory pathway that controls body temperature. *Nat Neurosci.* 2008;11(1):62–71.
- [36] Cao WH, Madden CJ, Morrison SF. Inhibition of brown adipose tissue thermogenesis by neurons in the ventrolateral medulla and in the nucleus tractus solitarius. *Am J Physiol Regul Integr Comp Physiol.* 2010;299(1):R277–90.
- [37] Garami A, Shimansky YP, Pakai E, et al. Contributions of different modes of TRPV1 activation to TRPV1 antagonist-induced hyperthermia. *J Neurosci.* 2010;30(4):1435–1440.
- [38] Garami A, Pakai E, Oliveira DL, et al. Thermoregulatory phenotype of the *Trpv1* knockout mouse: thermoeffector dysbalance with hyperkinesia. *J Neurosci.* 2011;31(5):1721–1733.
- [39] Garami A, Ibrahim M, Gilbraith K, et al. Transient receptor potential vanilloid 1 antagonists prevent anesthesia-induced hypothermia and decrease postincisional opioid dose requirements in rodents. *Anesthesiology.* 2017;127(5):813–823.
- [40] Himms-Hagen J, Cui J, Danforth E Jr., et al. Effect of CL-316,243, a thermogenic beta 3-agonist, on energy balance and brown and white adipose tissues in rats. *Am J Physiol.* 1994;266(4 Pt 2):R1371–82.
- [41] Mund RA, Frishman WH. Brown adipose tissue thermogenesis: beta3-adrenoreceptors as a potential target for the treatment of obesity in humans. *Cardiol Rev.* 2013;21(6):265–269.
- [42] Nakamura K, Matsumura K, Kaneko T, et al. The rostral raphe pallidus nucleus mediates pyrogenic transmission from the preoptic area. *J Neurosci.* 2002;22(11):4600–4610.
- [43] Paxinos G, Watson C. *The Rat Brain in Stereotaxic Coordinates.* 4th San Diego: Academic Press; 1998.
- [44] Nakamura K, Matsumura K, Hubschle T, et al. Identification of sympathetic premotor neurons in medullary raphe regions mediating fever and other thermoregulatory functions. *J Neurosci.* 2004;24(23):5370–5380.
- [45] Simons CT, Kulchitsky VA, Sugimoto N, et al. Signaling the brain in systemic inflammation: which vagal branch is involved in fever genesis? *Am J Physiol.* 1998;275(1 Pt 2):R63–8.
- [46] Paxinos G, Watson C. *The Rat Brain in Stereotaxic coordinates.* 6th New York: Elsevier Academic Press; 2007.
- [47] Morrison SF, Nakamura K. Central mechanisms for thermoregulation. *Annu Rev Physiol.* 2019;81:285–308.
- [48] Sagar SM, Sharp FR, Curran T. Expression of c-fos protein in brain: metabolic mapping at the cellular level. *Science.* 1988;240(4857):1328–1331.
- [49] Hermes SM, Andresen MC, Aicher SA. Localization of TRPV1 and P2X3 in unmyelinated and myelinated vagal afferents in the rat. *J Chem Neuroanat.* 2016;72:1–7.
- [50] Schicho R, Florian W, Liebmann I, et al. Increased expression of TRPV1 receptor in dorsal root ganglia by acid insult of the rat gastric mucosa. *Eur J Neurosci.* 2004;19(7):1811–1818.
- [51] Janig W. Neurobiology of visceral afferent neurons: neuroanatomy, functions, organ regulations and sensations. *Biol Psychol.* 1996;42(1–2):29–51.
- [52] Spencer NJ, Zagorodnyuk V, Brookes SJ, et al. Spinal afferent nerve endings in visceral organs: recent advances. *Am J Physiol Gastrointest Liver Physiol.* 2016;311(6):G1056–63.
- [53] Jones MW, Apkarian AV, Stevens RT, et al. The spinothalamic tract: an examination of the cells of origin of the dorsolateral and ventral spinothalamic pathways in cats. *J Comp Neurol.* 1987;260(3):349–361.
- [54] Craig AD, Kniffki KD. Spinothalamic lumbosacral lamina I cells responsive to skin and muscle stimulation in the cat. *J Physiol.* 1985;365(1):197–221.
- [55] Norrsell U. Thermosensory defects after cervical spinal cord lesions in the cat. *Exp Brain Res.* 1979;35(3):479–494.

- [56] Stroman PW, Bosma RL, Tsyben A. Somatotopic arrangement of thermal sensory regions in the healthy human spinal cord determined by means of spinal cord functional MRI. *Magn Reson Med*. 2012;68(3):923–931.
- [57] Norrsell U. Behavioural thermosensitivity after bilateral lesions of the lateral funiculi in the cervical spinal cord of the cat. *Exp Brain Res*. 1989;78(2):374–379.
- [58] Norrsell U. Behavioural thermosensitivity after unilateral, partial lesions of the lateral funiculus in the cervical spinal cord of the cat. *Exp Brain Res*. 1989;78(2):369–373.
- [59] Laurin J, Pertici V, Dousset E, et al. Group III and IV muscle afferents: role on central motor drive and clinical implications. *Neuroscience*. 2015;290:543–551.
- [60] Ling LJ, Honda T, Shimada Y, et al. Central projection of unmyelinated (C) primary afferent fibers from gastrocnemius muscle in the Guinea pig. *J Comp Neurol*. 2003;461(2):140–150.
- [61] Light AR, Huguen RW, Zhang J, et al. Dorsal root ganglion neurons innervating skeletal muscle respond to physiological combinations of protons, ATP, and lactate mediated by ASIC, P2X, and TRPV1. *J Neurophysiol*. 2008;100(3):1184–1201.
- [62] Gao Z, Li JD, Sinoway LI, et al. Effect of muscle interstitial pH on P2X and TRPV1 receptor-mediated pressor response. *J Appl Physiol*. 2007;102(6):2288–2293.
- [63] Kark T, Bagi Z, Lizanecz E, et al. Tissue-specific regulation of microvascular diameter: opposite functional roles of neuronal and smooth muscle located vanilloid receptor-1. *Mol Pharmacol*. 2008;73(5):1405–1412.
- [64] Jin H, Sun P, Takatori S, et al. Involvement of perivascular nerves and transient receptor potential vanilloid 1 (TRPV1) in vascular responses to histamine in rat mesenteric resistance arteries. *Eur J Pharmacol*. 2012;680(1–3):73–80.
- [65] Scotland RS, Chauhan S, Davis C, et al. Vanilloid receptor TRPV1, sensory C-fibers, and vascular autoregulation: a novel mechanism involved in myogenic constriction. *Circ Res*. 2004;95(10):1027–1034.
- [66] Luo Z, Ma L, Zhao Z, et al. TRPV1 activation improves exercise endurance and energy metabolism through PGC-1 α upregulation in mice. *Cell Res*. 2012;22(3):551–564.
- [67] Nybo L, Rasmussen P, Sawka MN. Performance in the heat-physiological factors of importance for hyperthermia-induced fatigue. *Compr Physiol*. 2014;4(2):657–689.
- [68] Robergs RA, Ghiasvand F, Parker D. Biochemistry of exercise-induced metabolic acidosis. *Am J Physiol Regul Integr Comp Physiol*. 2004;287(3):R502–16.
- [69] Cho SJ, Vaca MA, Miranda CJ, et al. Inhibition of transient potential receptor vanilloid type 1 suppresses seizure susceptibility in the genetically epilepsy-prone rat. *CNS Neurosci Ther*. 2018;24(1):18–28.
- [70] Gram DX, Fribo J, Nagy I, et al. TRPV1 antagonists as novel anti-diabetic agents: regulation of oral glucose tolerance and insulin secretion through reduction of low-grade inflammation? *Med Sci (Basel)*. 2019;7(8):82.
- [71] Wanner SP, Garami A, Pakai E, et al. Aging reverses the role of the transient receptor potential vanilloid-1 channel in systemic inflammation from anti-inflammatory to proinflammatory. *Cell Cycle*. 2012;11(2):343–349.
- [72] Malek S, Sample SJ, Schwartz Z, et al. Effect of analgesic therapy on clinical outcome measures in a randomized controlled trial using client-owned dogs with Hip osteoarthritis. *BMC Vet Res*. 2012;8:185.
- [73] Cabanero D, Villalba-Riquelme E, Fernandez-Ballester G, et al. ThermoTRP channels in pain sexual dimorphism: new insights for drug intervention. *Pharmacol Ther*. 2022;240:108297.
- [74] Janssen I, Heymsfield SB, Wang ZM, et al. Skeletal muscle mass and distribution in 468 men and women aged 18–88 yr. *J Appl Physiol*. 2000;89(1):81–88.